JPP Journal of Pharmacy and Pharmacology

ROYAL PHARMACEUTICAL SOCIETY

JPP Journal of Pharmacy and Pharmacology

JPP 2011, 63: 1283–1289

Received February 18, 2011
Accepted July 4, 2011
DOI
10.1111/j.2042-7158.2011.01338.x
ISSN 0022-3573

Research Paper

# An investigation of the chick chorioallantoic membrane as an alternative model to various biological tissues for permeation studies

Stephanie Li Mei Tay, Paul Wan Sia Heng and Lai Wah Chan

Department of Pharmacy, National University of Singapore, Singapore

## Abstract

**Objectives** The chick chorioallantoic membrane (CAM) was explored as a biological membrane for use in the study of drug permeation with a Franz diffusion cell.

**Methods** The CAM was removed from fertilized chicken eggs of embryo age 9–18 days. The permeation profiles of nicotine through the fresh CAM were first obtained with a Franz diffusion cell. The permeation profiles of nicotine through frozen CAM, snake skin, pig skin, pig retina and pig buccal mucosa were also determined and compared with those of the fresh CAM.

**Key findings** The permeability coefficient of the CAM varied with its age. The CAM at embryo age 13 was the most robust, showing the lowest standard error in permeability. It was thus chosen for comparative studies with snake skin, pig skin, retina and buccal mucosa. The CAM was found to be most similar to the buccal mucosa in terms of permeation profile and permeability coefficient values. Frozen CAM was also found to have a higher permeability coefficient than fresh CAM. The enhanced permeability was attributed to freezing, which affected the integrity of the CAM structure.

**Conclusions** From the findings, CAM shows potential as an alternative to the pig buccal mucosa as an in-vitro buccal model. The robustness of the CAM for drug permeation studies is affected by its age.

**Keywords** buccal mucosa; chick chorioallantoic membrane; permeation

## Introduction

### Chick choriollantoic membrane

The chorioallantoic membrane (CAM) is also known as the chorioallantois and is derived from two extra-embryonic membranes: the chorion and allantois. The chorion and allantois start to fuse together to form the CAM at about 4 days after the egg is laid.[1] The day the egg is laid is known as embryo age (EA) 0.

Besides being a respiratory and excretory organ, the CAM provides support to the underlying extra-embryonic blood vessels such as the vitelline vessels found on the surface of the yolk. The CAM is also involved in the transport of sodium and chloride from the allantoic sac, which is located close to the amnion sac, and calcium from the eggshell to the vasculature.

Histologically, the CAM consists of three layers: ectoderm, mesoderm and endoderm.[2] In addition to angiogenic, vasoreactivity and irritancy studies,[3–7] the CAM has also been used as a model for the human skin,[8] eye[9] and endocrine system.[10]

Angiogenesis and irritancy studies have involved the application of test substances on the CAM surface. The change in vessel density and vessel growth are determined in angiogenesis studies,[3,4] whilst vessel damage is assessed in the evaluation of irritancy.[5–7] Skin grafts have been placed on the CAM when used as a model for human skin.[8] The reaction of the CAM to irritants has been used as an alternative to the Draize test to predict ocular irritation.[9] The influence of environmental factors on the CAM has been studied to indicate the effects of ecological changes on the endocrine system.[10]

The CAM has been extensively used and it is of interest to employ it as an in-vitro model for drug permeation studies because chicken eggs are markedly easy to obtain and use. Hence the aim of the study was to compare the permeation profile of a model drug between the CAM and other biological membranes, to assess its suitability as a biological membrane

**Correspondence:** Lai Wah Chan, Department of Pharmacy, National University of Singapore, No.18 Science Drive 4, Block S4, Singapore 117543. E-mail: phaclw@nus.edu.sg

for permeation studies. The other biological membranes studied are commonly used to represent human tissue: snake and pig skin were used to represent human skin whilst pig buccal mucosa and retina tissue represented human buccal mucosa and retina tissue, respectively. As tissues are usually preserved in the freezer, this study also determined the influence of freezing on the CAM tissue. Nicotine was used as the model drug as it possesses good solubility in both polar and non-polar solvents. Its low molecular weight does not represent a limiting factor to drug permeation,[11] hence it is suitable for assessing the influence of the various biological membranes on drug permeation.

## Materials and Methods

### Materials

Freshly laid, fertilized specific pathogen-free (SPF) chicken eggs of the *White Leghorn* strain were purchased from Chew's Agriculture, Singapore. The *White Leghorn* strain is commonly used for experiments. L-nicotine (>99%, Acros Organics, USA) was used as a model drug. Shed skin of the King Cobra, *Ophiophagus Hannah,* was a gift from Khon Kaen University, Thailand. Pig abdominal skin, buccal mucosa as well as retina tissue were obtained from 4-month-old Yorkshire-Duroc mix breed female pigs (Animal Holding Unit, National University of Singapore). Disodium hydrogen orthophosphate dodecahydrate (BDH Chemicals, England), sodium dihydrogenphosphate dehydrate (Nacalai Tesque, Japan) and sodium chloride (Merck Germany) were used to prepare isotonic phosphate buffer.

Approval from the Institutional Animal Care and Use Committee (National University of Singapore) was obtained for CAM older than EA 10.

### Methods

#### *Preparation of membranes for study*

##### *Cellulose membrane*

A membrane composed of regenerated cellulose (Sartorius Stedim Biotech, France) was used to support the test biological membrane in the Franz diffusion cell. The cellulose membrane, with a pore size of 0.45 μm, was cut into a circular disc of diameter 34 mm. The test biological membrane was placed on top of the cellulose membrane.

##### *CAM*

The eggs were incubated at 37°C for different periods of time to produce CAM of different embryonic age. The CAM was harvested by first making a hole at the blunt end of the egg with a sharp pair of forceps. The eggshell was then cut in half along its length and the contents of the egg emptied, leaving the CAM adhered to the underside of the shell beneath the inner shell membrane. Normal saline was used to wash the surface of the CAM, after which the CAM was carefully removed from the inner shell membrane with a pair of forceps. The CAM was rinsed in normal saline again and immediately used in the permeation study or frozen for use at a later date. The thickness of the CAM was also measured with a micrometer at at least three different locations, and the measurements were averaged.

##### *King Cobra skin*

The shed King Cobra skin was washed and dried at room temperature before being cut into discs and stored at room temperature. The skin discs were hydrated by soaking in isotonic phosphate buffer in a covered Petri dish for 30 min prior to use.

##### *Pig skin*

Freshly harvested pig skin was frozen at −30°C and thawed prior to preparation. The hair on the skin was trimmed with a pair of scissors. The skin was then cut into appropriate sizes, rinsed with normal saline and soaked in isotonic phosphate buffer for 30 min prior to use.

#### Pig buccal mucosa

The sample supplied consisted of the buccal mucosa with underlying fat and muscle tissue. Because of this the specimen was first treated by soaking in hot water at 60°C for 2 min to facilitate the removal of the mucosal layer from the base material tissue with a pair of forceps. The buccal mucosa was cut into appropriate sizes, washed with normal saline and soaked in isotonic phosphate buffer for 30 min prior to use.

#### Pig retina tissue

The retina tissue was carefully removed from the back of the pig eyeball using a pair of forceps. The retinal tissue was then washed with normal saline and soaked in isotonic phosphate buffer for 30 min prior to use.

#### Permeation study

Permeation studies were carried out with the use of the Hanson Microette® apparatus (Hanson Research, USA), which consists of six Franz diffusion cells in a vertical arrangement. Each diffusion cell consists of a lower receptor compartment and an upper donor compartment, jacketed at 37°C and connected by a central orifice of diameter 15 mm. The test membrane, with an underlying supporting cellulose membrane, was placed on a Teflon disk with a central orifice of diameter 8 mm or 15 mm and clamped between the donor and receptor compartments. The donor compartment was filled with 1 ml of drug solution while the receptor compartment was filled to its capacity with 7 ml of isotonic phosphate buffer. Sampling using a vacuum-controlled autosampler was conducted over pre-determined time intervals. Sink conditions were maintained with the continuous use of a helix stirrer set at 600 rpm, topped-up with fresh isotonic phosphate buffer in the receptor compartment following sample withdrawal. The samples collected were analysed by HPLC. The permeation study was carried out in triplicate.

#### HPLC analysis

The quantification of nicotine was performed with reversed-phase HPLC using a C-18 column (Hypersil, 5 μm, 4.6 mm × 200 mm). The mobile phase consisted of 0.05 M sodium acetate and methanol in the proportion of 88 : 12 v/v, with 0.5% v/v triethylamine. The pH of the mobile phase was then adjusted with glacial acetic acid to pH 4.2. The flow rate was set at 1 ml/min with sample injection volume of 20 μl and nicotine was assayed spectrophotometrically at 259 nm.

Under these conditions, the calibration plot for nicotine between 0.0005 and 0.2% v/v demonstrated good linearity and reproducibility ($r^2$ >0.99).

### Data analysis

Sink conditions were maintained in the receptor compartment. As such, the amount of drug that permeated through the membrane can be described by Equation 1.[12])

$$M_T[n] = V_r \cdot C[n] + V_s \cdot \sum_{i=1}^{i=n-1} \{C[n-1]\} \quad (1)$$

where $M_T[n]$ is the cumulative amount of drug transported across the membrane at time $t$, $C[n]$ is the concentration of drug in the receptor medium at time $t$, $V_r$ is the volume of the receptor medium, $V_s$ is the volume of sample removed for analysis at each sampling point and $\Sigma\{C[n-1]\}$ denotes the summation of the previously measured concentrations.

Steady-state flux can be determined by Fick's first law of diffusion, which is descriptive of the steady-state diffusion through a membrane (Equation 2).

$$J = \frac{dQ}{dt}\frac{1}{A} = K_p C_D \quad (2)$$

where $J$ is the steady-state flux, $Q$ is the amount of drug that permeates through the membrane, $t$ is the exposure time, $A$ is the area of application, $K_p$ is the permeability coefficient and $C_D$ is the concentration of drug applied.

The cumulative amount of drug that permeated through the membrane per unit area $Q/A$ was calculated and plotted as a function of time, $t$. Steady-state flux $J$ was obtained by linear regression analysis of the initial linear portion of the plot. The $K_p$ value was obtained by dividing the steady-state flux value by the concentration of drug applied.

### Statistical analysis

Statistical analysis of the permeability coefficients of nicotine through the CAM, pig skin, snake skin, buccal mucosal and retinal tissue was performed using the Kruskal–Wallis test (SPSS, Version 11, Lead Technologies, USA). A significance level of $P < 0.05$ denoted significance in all cases.

## Results

The total duration of experimentation was varied as preliminary investigations showed that the pig skin and snake skin required a longer time for nicotine to permeate compared to the other biological tissues. Hence a longer experimental time was allowed for the pig skin and snake skin. The other biological membranes were found to reach maximum permeation in a much shorter time and the experimental time was correspondingly shortened.

### Cellulose membrane

In a separate control study, the cellulose membrane was used without any biological membrane to determine its effect on drug permeation. The amount of nicotine that permeated through the cellulose membrane was rapid, reaching a plateau in less than an hour (Figure 1). The high permeation rate clearly demonstrates minimal permeation resistance caused by the cellulose membrane. Results obtained for the cellulose membrane showed a smaller variation compared to the biological membranes. Being synthetic, the cellulose membrane has precise composition, unlike the biological membranes, which have slightly variable composition.

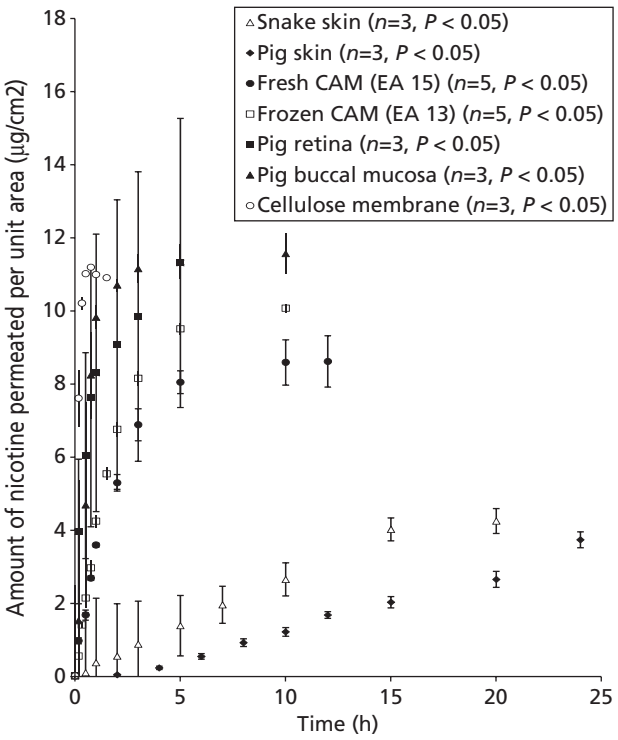


**Figure 1** Permeation profiles of nicotine through different membranes. Values shown are expressed as mean ± SEM.

### Permeation profile of fresh CAM

The typical permeation profile of nicotine through the CAM is depicted in Figure 1. Irrespective of embryo age, the total amount of nicotine that permeated through the CAM reached a plateau after about 5 h. The CAM thickness increased linearly with embryo age ($r^2 = 0.94$) (Figure 2). The permeation coefficient was found to vary with embryo age ($P < 0.05$) (Table 1). This suggests that the composition of the CAM, which varied with age, had some effect on drug permeation.

The change in $K_p$ values with embryo age could be roughly accounted for by the morphological change of the ectoderm (Table 1). The $K_p$ value of fresh CAM decreased after EA 11 and reached a minimum at EA 13 before increasing at EA 14, decreasing at EA 15, increasing again at EA 16 and finally reaching a plateau at EA17 and EA 18 (Figure 3). However, the $K_p$ values from EA 15 to EA 18 can be regarded as almost similar because of the overlapping standard errors.

### Frozen CAM

The permeation profile of nicotine through the frozen CAM at EA 13 is shown in Figure 1 and the permeability

coefficients of the frozen CAM at EA 9 to EA 18 are shown in Table 1. In comparison with the permeation of fresh CAM, the amount of nicotine that permeated through the frozen CAM was significantly higher ($P < 0.05$) at each corresponding fresh CAM of the same EA (Table 1). However, the plot of $K_p$ vs EA for fresh and frozen CAM showed similar trends (Figure 3). The minima in permeation were observed around EA 13–14.

## Permeation studies using animal tissues

The permeation profile of nicotine through pig skin shows that the total amount of permeated nicotine was lower than in fresh and frozen CAM. In addition, it took a longer time for nicotine to reach a plateau in pig skin than in the CAM (Figure 1). Permeation through snake skin was slower than in the other biological membranes. The rate of permeation of nicotine is in

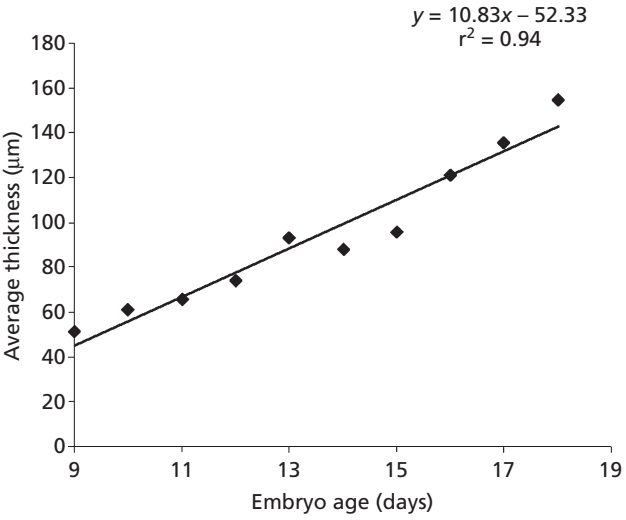


**Figure 2** Average thickness of CAM at different embryo age.

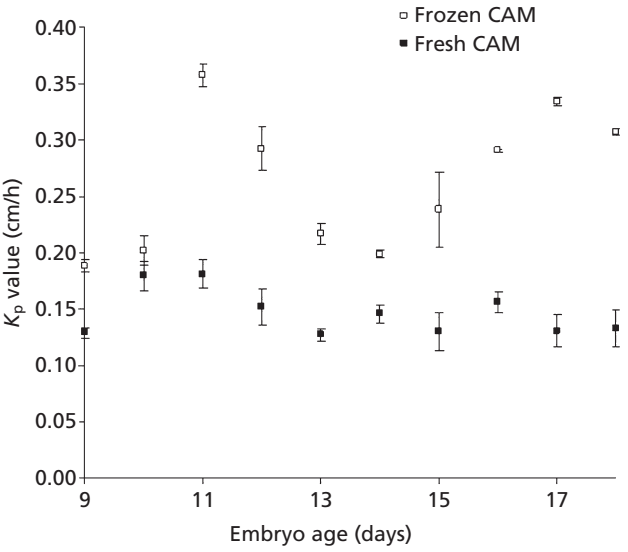


**Figure 3** Plots of EA vs $K_p$ for nicotine through frozen and fresh CAMs.

**Table 1** $K_p$ values of test membranes with nicotine

| | Embryo age | Permeability coefficient, $K_p$ | *P* value | Standard error of mean | Coefficient of variance |
|---|---|---|---|---|---|
| Fresh CAM | 9 | 0.129 | <0.05 | 0.0029 | 4.98 |
| ($n = 5$) | 10 | 0.180 | <0.05 | 0.0128 | 15.9 |
| | 11 | 0.181 | <0.05 | 0.0143 | 17.7 |
| | 12 | 0.152 | <0.05 | 0.0160 | 23.5 |
| | 13 | 0.127 | <0.05 | 0.0062 | 10.9 |
| | 14 | 0.170 | <0.05 | 0.0222 | 29.2 |
| | 15 | 0.130 | <0.05 | 0.0167 | 28.7 |
| | 16 | 0.156 | <0.05 | 0.0103 | 14.8 |
| | 17 | 0.130 | <0.05 | 0.0144 | 24.8 |
| | 18 | 0.132 | <0.05 | 0.0125 | 21.2 |
| Frozen CAM | 9 | 0.188 | <0.05 | 0.0043 | 5.06 |
| ($n = 5$) | 10 | 0.202 | <0.05 | 0.0104 | 11.5 |
| | 11 | 0.357 | <0.05 | 0.0072 | 4.53 |
| | 12 | 0.292 | <0.05 | 0.0148 | 11.3 |
| | 13 | 0.217 | <0.05 | 0.0074 | 7.58 |
| | 14 | 0.199 | <0.05 | 0.0026 | 2.96 |
| | 15 | 0.238 | <0.05 | 0.0259 | 24.3 |
| | 16 | 0.291 | <0.05 | 0.0009 | 0.758 |
| | 17 | 0.334 | <0.05 | 0.0032 | 2.12 |
| | 18 | 0.307 | <0.05 | 0.0026 | 1.86 |
| Snake skin ($n = 3$) | – | 0.011 | <0.05 | 0.0023 | 36.8 |
| Pig skin ($n = 3$) | – | 0.003 | <0.05 | 0.0002 | 13.4 |
| Pig retina ($n = 3$) | – | 0.473 | <0.05 | 0.1580 | 57.9 |
| Pig buccal mucosa ($n = 3$) | – | 0.133 | <0.05 | 0.0362 | 47.1 |
| Cellulose membrane ($n = 3$) | – | 1.777 | <0.05 | 0.1280 | 12.5 |

agreement with the findings from a previous study.[13] The $K_p$ value of the snake skin was significantly lower than those of fresh and frozen CAM but higher than that of pig skin as the shed snake skin was considerably thinner and had no underlying tissues.

The organs and membranes of pigs have been considered to be structurally similar to their counterparts in humans. However, the permeation profile of nicotine through retina tissue showed that the total amount of permeated nicotine was significantly higher than those for fresh and frozen CAMs. In fact, the average $K_p$ value of the retina was the highest among the biological membranes tested. For the buccal mucosa, nicotine permeation was markedly higher than through fresh CAM. However, the $K_p$ values of the buccal mucosa and fresh CAM were comparable. The pig buccal mucosa in this study was found to be 44 times more permeable than the pig skin, which is widely used as a human skin model.

## Discussion

### Cellulose membrane

The function of the cellulose membrane was to provide support to the test biological membrane placed across the orifice between the donor and receptor compartments. Hydrophobic membranes were avoided as they were found to be poorly wetted by the aqueous media used. Poor wetting of the membrane was found to affect the permeation of nitroglycerin.[14] The cellulose membrane used was easily wetted, mechanically strong when wetted and did not pose any significant barrier to drug permeation. Hence, it did not hinder or alter the rate of nicotine permeation through the biological membranes studied.

### Permeation profile using fresh CAM

The change in $K_p$ values with embryo age could be roughly accounted for by the morphological changes of the ectoderm. The CAM consists of three layers: the ectoderm, mesoderm and endoderm. These grow at different rates and exhibit different morphological characteristics. The ectoderm is made up of a majority of cuboidal cells while the mesoderm consists of blood vessels and cells with fibrillar material. The endoderm consists of squamous and cuboidal cells. As the egg matures, these cells change to columnar type and large intercellular spaces appear after EA 16. Light and electron microscopy have shown that the ectoderm layer is the densest, with closely packed cells. The ectoderm layer is therefore likely to be the greatest barrier to permeation. After EA 10, the ectoderm proliferates non-uniformly until it is at least eight cells thick. It reaches maximum thickness around EA 14, then degrades after EA 15. As such, a gradual decrease in $K_p$ after EA 10 and minima around EA 14 were observed. Some deviation from the expected trend suggests that the mesoderm and endoderm also affected the permeation of nicotine, but to smaller extents (Figure 3). There was an increase in the thickness of the endothelium of the larger blood vessels in the mesoderm after EA 15.[1,15] This increase in thickness of the endothelium may represent a barrier to permeation and could account for the lower $K_p$ values that were observed after EA 14 instead of the expected increase (Figure 3). The consistency of $K_p$ values from EA 15 to EA 18 suggests that CAM of EA 15 is suitable for use as a permeation model.

### Frozen CAM

It should be optimal to employ fresh CAM in experiments as it has been found that freshly harvested animal skin retains most of the characteristics of living skin.[16] Availability of fresh CAM is not always possible or convenient but the CAMs of certain EA (EA 13 to EA 18) may be frozen prior to future use at the desired time point. The properties of frozen CAM in comparison with fresh CAM were therefore investigated to examine the effect of freezing on the permeation of nicotine.

Statistically significant differences in flux values between fresh and frozen porcine buccal mucosa have been reported.[17] Freezing has also been found to cause an increase in permeability of the skin.[18–21] This was attributed to the formation of ice crystals in the skin as well as disorganization of lipids, damaging the keratinocytes and lipid matrix of the rate-limiting stratum corneum. Mechanical damage and osmotic effects have also been proposed as possible mechanisms of increased membrane permeability.[22]

Although fresh CAM may be ideal it may not always be available. Hence frozen CAM is a viable alternative for permeability studies.

### Pig skin

Pig skin is regarded as one of the best animal models for human skin.[23,24] The $K_p$ value obtained for pig skin was similar to that obtained from other studies that compared pig skin to human skin.[25]

The $K_p$ value of the pig skin was significantly lower than those of fresh and frozen CAMs but similar to the $K_p$ value of 0.0039 cm/h for human skin.[26] This indicates that the permeation profile through pig skin resembles that of human skin, but not the CAM. Hence, the CAM is not suitable as a skin model. The metabolizing capabilities of the skin are largely attributed to the viable epidermis.[27] In this case, the pig skin was frozen prior to use and the tissue was not viable, hence metabolism of nicotine could not have occurred. The stratum corneum is 13–17 μm thick, consisting of 10–20 layers of keratin-rich corneocytes and lipid layers. The corneocytes are embedded in an extracellular lipid matrix that is arranged in an orderly manner. This complex arrangement of corneocytes and lipids is referred to as the brick and mortar model and is the main barrier to drug permeation through the skin.[28]

A full thickness specimen of pig skin was used in the present study. The stratum corneum of the pig skin may have represented a permeation barrier and accounted for the significantly lower amount of nicotine that permeated through as compared to the CAM, which does not possess the keratinized stratum corneum.

### Snake skin

Snake skin is easily available without causing harm to the snake as a relatively large amount of skin is periodically shed from each snake. Shed snake skin consists of three layers without any hair follicles. The outermost layer is rich in $\beta$-keratin while the innermost layer is rich in $\alpha$-keratin. The intermediate mesos layer, which is composed of three to five sub-layers of cornified cells enclosed by intercellular lipids,

closely resembles the stratum corneum of the human skin. The vascular structures and collageneous connective tissues found in snake and human skin are also similar.[29] Snake skin has therefore been used as a model for human skin.[30] The $K_p$ value obtained for snake skin was higher than that for pig skin. This could be attributed to the thicker rate-limiting stratum corneum layer found in pig skin (26.4 ± 0.4 μm) as compared to that of snake skin (10–20 μm).[25,31] Nevertheless, the snake skin is a better model for the human skin than CAM.

### Retina tissue

The retinal pigment epithelium and endothelial membrane of the retinal vessels possess tight junctions that are non-leaky.[32] The CAM is of comparable thickness to human retina at approximately 100–300 μm. Furthermore, the tissue responses of CAM used in in-vitro studies have been found to be similar to those of rabbit retina in in-vivo studies.[33] It should be pointed out that the retina is a very delicate piece of tissue that is easily damaged. The high $K_p$ value and large coefficient of variance strongly suggest that the retinal tissue was partially damaged in the preparation procedure, albeit in a manner not visible to the naked eye. The random damaged spots on the retina facilitated permeation of the drug through the tissue to markedly different extents. Close observation of the retinal samples revealed non-uniform distribution of retinal pigment. The process of removing the retina and soaking it in isotonic phosphate buffer resulted in some loss of the retinal pigmented epithelium. The retinal pigmented epithelium has tight junctions, which have been reported to form a barrier to permeation of compounds through the retina.[34] Possible higher nicotine permeation through the retina therefore resulted, showing higher $K_p$ values with large coefficient of variance. Nevertheless, the findings suggest that the CAM can be akin to the retinal epithelium. Expertise in harvesting the retina or cornea could be improved with more practice.

### Buccal tissue

The buccal mucosa is suitable for the delivery of macromolecules and hydrophilic compounds.[35] The pig buccal mucosa is commonly used as an alternative to human buccal mucosa in the study of drug delivery by the buccal route.[36] Cell cultures of human buccal mucosa are available but there have been few studies on them and information is limited. Rabbit and hamster buccal mucosa are less desirable because of the patchy keratinization of the tissue and their limited size.[37] Although the average thickness of the buccal mucosa is 500–600 μm, and much thicker than the CAM,[38] the similarity between CAM and buccal mucosa permeation coefficients raises the possibility of the CAM being used as a substitute for human buccal mucosa instead of pig buccal mucosa. CAM as a human buccal model has many advantages over the pig buccal mucosa. There is the possibility of tissue damage to the buccal mucosa that may occur when the pig masticates and accidentally bites the buccal mucosa. The CAM is kept in a protected environment in the egg, away from physical assaults from the environment. Tissue acquisition from pigs is also a more laborious and time-intensive procedure compared to harvesting the CAM. More costs are incurred with the raising of pigs to a suitable age for experimentation and their sacrifice in a humane manner. Most importantly, there are less ethical issues surrounding the use of CAM and this makes it an excellent in-vivo or in-situ membrane model.

## Conclusion

The CAM was more similar to the buccal mucosa as opposed to keratinized skin in terms of permeation profile and permeability coefficient values. Fresh and frozen CAMs displayed similar permeation profiles but frozen CAM was found to be more permeable than fresh CAM. The CAM shows potential as an alternative biological membrane to the pig buccal mucosa. It can be used as a buccal model in the evaluation of absorption of drugs that are administered through the buccal route. The CAM is also potentially useful as a model for corneal or retinal epithelium.

## Declarations

### Conflict of interest

The Authors declare that they have no conflicts of interest to disclose.

### Funding

This work was supported by the National Medical Research Council, NMRC/1187/2008 (R-148-000-114-213) Singapore and the National University of Singapore Academic Research Fund (R-148-000-085-112).

## References

1. Romanoff AL. *The Avian Embryo; Structural and Functional Development*. New York: The Macmillan Company, 1960.
2. Fuchs A, Lindenbaum ES. The two- and three-dimensional structure of the microcirculation of the chick chorioallantoic membrane. *Acta Anat (Basel)* 1988; 131: 271–275.
3. Forough R *et al*. Cell-based and direct gene transfer-induced angiogenesis via a secreted chimeric fibroblast growth factor-1 (sp-FGF-1) in the chick chorioallantoic membrane (CAM). *Angiogenesis* 2003; 6: 47–54.
4. Richardson M *et al*. Inhibition by doxycycline of angiogenesis in the chicken chorioallantoic membrane (CAM). *Cancer Chemother Pharmacol* 2005; 56: 1–9.
5. Dunn LK *et al*. Chick chorioallantoic membrane as an in vivo model to study vasoreactivity: characterization of development-dependent hyperemia induced by epoxyeicosatrienoic acids (EETs). *Anat Rec A Discov Mol Cell Evol Biol* 2005; 285: 771–780.
6. Daston GP, McNamee P. *Alternatives to Toxicity Testing in Animals: Challenges and Opportunities*. [Environmental Health Perspectives – Online monthly journal of peer-reviewed research] 2005 Nov 2005 [cited September 2005].
7. Vinardell MP, Garcia L. The quantitative chorioallantoic membrane test using trypan blue stain to predict the eye irritancy of liquid scintillation cocktails. *Toxicol In Vitro* 2000; 14: 551–555.
8. Kunzi-Rapp K *et al*. Characterization of the chick chorioallantoic membrane model as a short-term in vivo system for human skin. *Arch Dermatol Res* 1999; 291: 290–295.
9. Debbasch C *et al*. Eye irritation of low-irritant cosmetic formulations: correlation of in vitro results with clinical data and product composition. *Food Chem Toxicol* 2005; 43: 155–165.

10. Cobb GP *et al*. Using chorioallantoic membranes for non-lethal assessment of persistent organic pollutant exposure and effect in oviparous wildlife. *Ecotoxicology* 2003; 12: 31–45.
11. Zorin S *et al*. In vitro test of nicotine's permeability through human skin. Risk evaluation and safety aspects. *Ann Occup Hyg* 1999; 43: 405–413.
12. Baker ND *et al*. The percutaneous absorption of *m*-azidopyrimethamine: a soft antifolate for topical use. *Int J Pharm* 1990; 65: 115–125.
13. Pongjanyakul T *et al*. Shed king cobra and cobra skins as model membranes for in-vitro nicotine permeation studies. *J Pharm Pharmacol* 2002; 54: 1345–1350.
14. Shargel LW-P *et al*., eds. *Applied Biopharmaceutics and Pharmacokinetics*, 5th edn. USA: The McGraw-Hill Companies, 2005.
15. Shumko JZ *et al*. Vascular histodifferentiation in the chick chorioallantoic membrane: a morphometric study. *Anat Rec* 1988; 220: 179–189.
16. Yazdanian M. The effect of freezing on cattle skin permeability. *Int J Pharmaceutics* 1994; 103: 93–96.
17. Van Eyk AD, Van der Biijl P. Comparative permeability of fresh and frozen/thawed porcine buccal mucosa towards various chemical markers. *SADJ* 2006; 61: 200–203.
18. Ahlstrom LA *et al*. The effects of freezing skin on transdermal drug penetration kinetics. *J Vet Pharmacol Ther* 2007; 30: 456–463.
19. Babu RJ *et al*. The influence of various methods of cold storage of skin on the permeation of melatonin and nimesulide. *J Control Release* 2003; 86: 49–57.
20. Kemppainen BW *et al*. Effects of skin storage-conditions and concentration of applied dose on [H-3] T-2 toxin penetration through excised human and monkey skin. *Food Chem Toxicol* 1986; 24: 221–227.
21. Swarbrick J *et al*. Drug permeation through human-skin. 1. Effect of storage-conditions of skin. *J Invest Dermatol* 1982; 78: 63–66.
22. Schafer AT, Kaufmann JD. What happens in freezing bodies? Experimental study of histological tissue change caused by freezing injuries. *Forensic Sci Int* 1999; 102: 149–158.
23. Barbero AM, Frasch HF. Pig and guinea pig skin as surrogates for human in vitro penetration studies: a quantitative review. *Toxicol In Vitro* 2009; 23: 1–13.
24. Lin SY *et al*. Comparisons of different animal skins with human skin in drug percutaneous penetration studies. *Methods Find Exp Clin Pharmacol* 1992; 14: 645–654.
25. Maibach HI, Bronaugh RL. *Topical Absorption of Dermatological Products*. New York: Marcel Dekker, 2002.
26. Berner B *et al*. A transdermal nicotine system: feasibility studies. *J Control Release* 1992; 20: 13–19.
27. Zwadlo-Klarwasser G *et al*. The chorioallantoic membrane of the chick embryo as a simple model for the study of the angiogenic and inflammatory response to biomaterials. *J Mater Sci Mater Med* 2001; 12: 195–199.
28. Dupuis D *et al*. In vivo relationship between horny layer reservoir effect and percutaneous absorption in human and rat. *J Invest Dermatol* 1984; 82: 353–356.
29. Godin B, Touitou E. Transdermal skin delivery: predictions for humans from in vivo, ex vivo and animal models. *Adv Drug Deliv Rev* 2007; 59: 1152–1161.
30. Takahashi K, Rytting JH. Novel approach to improve permeation of ondansetron across shed snake skin as a model membrane. *J Pharm Pharmacol* 2001; 53: 789–794.
31. Itoh T *et al*. Use of shed snake skin as a model membrane for invitro percutaneous penetration studies – comparison with human skin. *Pharm Res* 1990; 7: 1042–1047.
32. Cunhavaz JG. Blood-retinal barriers in health and disease. *Trans Ophthalmol Soc U K* 1980; 100: 337–340.
33. Leng T *et al*. The chick chorioallantoic membrane as a model tissue for surgical retinal research and simulation. *Retina* 2004; 24: 427–434.
34. Duvvuri S *et al*. Drug delivery to the retina: challenges and opportunities. *Expert Opin Biol Ther* 2003; 3: 45–56.
35. Tanojo H *et al*. In vivo human skin permeability enhancement by oleic acid: a laser Doppler velocimetry study. *J Control Release* 1999; 58: 97–104.
36. Obradovic T, Hidalgo IJ. In vitro models for investigations of buccal drug permeation and metabolism. In: Ehrhardt C, Kim K, eds. *Drug Absorption Studies: In Situ, In Vitro and In Silico Models*. New York: Springer, 2008: 167–181.
37. Tavakoli-Saberi MR, Audus KL. Cultured buccal epithelium: an in vitro model derived from the hamster pouch for studying drug transport and metabolism. *Pharm Res* 1989; 6: 160–166.
38. Nicolazzo JA *et al*. Enhancing the buccal mucosal uptake and retention of triamcinolone acetonide. *J Control Release* 2005; 105: 240–248.